arXiv:cond-mat/0309015v3 [cond-mat.dis-nn] 12 Apr 2005

Comparative numerical study of Anderson localisation in disordered electron systems

Gerald Schubert[1], Alexander Weiße[2], Gerhard Wellein[3], and Holger Fehske[1]

[1] Ernst-Moritz-Arndt-Universität Greifswald, Institut für Physik, Domstr. 10a, D-17489 Greifswald, Germany
[2] School of Physics, The University of New South Wales, Sydney, NSW 2052, Australia
[3] Regionales Rechenzentrum Erlangen (RRZE), Martensstraße 1, D-91058 Erlangen, Germany

Summary. Taking into account that a proper description of disordered systems should focus on distribution functions, the authors develop a powerful numerical scheme for the determination of the probability distribution of the local density of states (LDOS), which is based on a Chebyshev expansion with kernel polynomial refinement and allows the study of large finite clusters (up to 100^3). For the three-dimensional Anderson model it is demonstrated that the distribution of the LDOS shows a significant change at the disorder induced delocalisation-localisation transition. Consequently, the so-called typical density of states, defined as the geometric mean of the LDOS, emerges as a natural order parameter. The calculation of the phase diagram of the Anderson model proves the efficiency and reliability of the proposed approach in comparison to other localisation criteria, which rely, e.g., on the decay of the wavefunction or the inverse participation number.

1 Introduction

The localisation of quantum particles in disordered systems is one of the most intensively studied problems in condensed matter physics [1–5]. In real systems disorder can arise for a number reasons. We may think of randomly distributed impurities, vacancies or dislocations in an otherwise ideal crystal, of random arrangements of electronic or nuclear spins, etc. While the disorder appears in many forms that are sometimes difficult to characterise theoretically, the randomness in the model introduced and discussed by Anderson is simple but sufficient to capture the basic features of the disorder-induced metal insulator transition [6]. The Anderson Hamiltonian,

$$H = -t \sum_{\langle ij \rangle} \left[c_i^\dagger c_j + \text{H.c.} \right] + \sum_{j=1}^{N} \epsilon_j c_j^\dagger c_j \,, \tag{1}$$

describes noninteracting electrons moving on a lattice with random on-site potentials (compositional disorder). The operators $c_j^\dagger$ (c_j) create (annihilate) an electron in

a Wannier state centred at site j, and the local potentials ϵ_j are assumed to be independent, uniformly distributed random variables,

$$p(\epsilon_j) = \frac{1}{W}\,\theta\left(\frac{W}{2} - |\epsilon_j|\right) . \tag{2}$$

The parameter W is a measure for the strength of disorder and is usually given in units of the nearest neighbour hopping matrix element t. Throughout this work we consider d-dimensional hyper-cubic lattices with $N = L^d$ sites, impose periodic boundary conditions (PBC), and set the lattice spacing equal to unity.

The spectral properties of the Anderson model (1) have been carefully analysed (see, e.g., Ref. [7]). For sufficiently large disorder or near the band tails, the spectrum consists exclusively of discrete eigenvalues, and the corresponding eigenfunctions are exponentially localised. Since localised electrons do not contribute to the transport of charge or energy, the energy that separates localised and extended eigenstates is called the mobility edge. For any finite disorder $W > 0$, on a one-dimensional (1d) lattice, all eigenstates of (1) are localised [8,9]. This is believed to hold also in 2d, where the existence of a transition from localised to delocalised states at finite W would contradict the one parameter scaling theory [10,11].

In spite of the progress made over the last decades, the Anderson metal-insulator transition is still not completely understood. There are several reasons why the existing theories remain unsatisfactory. Especially when electron-electron or electron-phonon interactions come into play, the very successful one-parameter scaling approach might be problematic, because close to the localisation transition the energy scales associated with both disorder and interactions are comparable to the Fermi energy [12]. On the other hand, the numerical study of the localisation-delocalisation transition is demanding, since the involved length scales can become extraordinary large, in particular near the critical point. Obviously, methods that are based on a full diagonalisation of the Hamiltonian and on the study of the one-particle eigenstates are restricted to rather small systems. Examples are the calculation of the localisation length from the decay of the electronic wavefunction or the evaluation of the inverse participation number. In addition, one-particle eigenstates are not defined for interacting systems. Hence, none of these criteria can easily be generalised to interacting disordered systems. To overcome these difficulties is perhaps the most challenging issue of current research on disordered materials.

Motivated by this situation, this contribution provides a (quasi approximation free) numerical analysis of the recently revived "local order parameter" approach to the Anderson transition, which, within the framework of the statistical dynamical mean field approximation, has been successfully applied also to correlated electron (phonon) systems [12,14]. Adopting a local point of view and focusing on the distribution of the physically interesting quantities, the method follows the original route to the localisation problem established by Abou-Chacra et al. [16]. In particular, we demonstrate that for Anderson type models the distribution of the local density of states (LDOS) can be determined very easily by the kernel polynomial method (KPM) [17], a refined Chebyshev expansion technique. Based on the distribution of the LDOS, localised states are distinguished from extended states by a vanishing geometrical average, which is usually called the "typical DOS". In addition, it turns out that this quantity characterises the disorder-induced metal-insulator transition also in more complex systems [12,14,19–22].

To examine the efficiency and accuracy of the proposed LDOS-KPM approach, we carry out a comparative numerical study of the localisation-delocalisation transition. In view of the wealth of known results, the 3d Anderson model seems to be best suited for this kind of investigation. The results we obtain for the mobility edge from different methods allow for a detailed understanding of the typical DOS concept and open the road towards an application to more complex situations.

2 Anderson transition

As the Anderson transition is expected only for $d > 2$, in this chapter we focus on the 3d case, for which the lack of successful analytical approaches necessitates a numerical treatment. In contrast to the widely used numerical transfer matrix method [23–25], which describes the 3d system as a quasi-1d system of finite cross section, below we stress the bulk properties of the system and consider cubic clusters which extend equally in all spatial directions. Due to the large length scales that emerge in the critical region, it is generally a difficult task to interpret the results of such finite cluster calculations.

As a kind of benchmarking, we review and compare established localisation criteria, namely, the localisation length (Sec. 2.1) and the inverse participation number (Sec. 2.2). Both can be extracted from the one-particle wavefunctions, which, however, requires the complete numerical diagonalisation of the Hamiltonian (1). In Sec. 2.3, we present the new approach that is based on the distribution of the LDOS. Since the calculation of the LDOS via the KPM requires only sparse matrix vector multiplications, this technique scales linearly with the number of lattice sites and permits the study of significantly larger systems.

2.1 Decay of the wavefunction

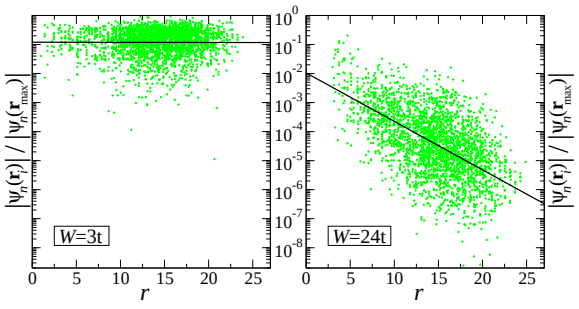


Fig.1 Decay of an electronic wavefunction ψ_n in the band centre as a function of the distance $r = |\mathbf{r}_i - \mathbf{r}_{\max}|$ to the site with maximum amplitude, $\mathbf{r}_{\max}$. Results are given each for one fixed energy and realization of disorder, $N = 30^3$, PBC.

The most obvious but costly way to access the localisation properties of an electronic wavefunction is the direct calculation of the localisation length λ, which is infinite for extended states and finite otherwise. For localised states, the envelope of the wavefunction decays exponentially from some point $\mathbf{r}_{\max}$ in the crystal.

$$|\psi_n(\mathbf{r}_i)| \sim f(\mathbf{r}_i) \exp\left(-\frac{|\mathbf{r}_i - \mathbf{r}_{\max}|}{\lambda}\right) . \tag{3}$$

The random function $f(\mathbf{r}_i)$ describes the statistical fluctuations of the amplitudes $\psi_n(\mathbf{r}_i)$ of the eigenfunction ψ_n at energy E_n. Given ψ_n, the localisation length $\lambda(E_n)$ is obtained by locating the site of maximum amplitude, $\mathbf{r}_{\max}$, and fitting Eq. (3) to the data. In contrast to the case of weak disorder, where the amplitude is essentially independent of the distance from $\mathbf{r}_{\max}$, at higher values of W a clear exponential decay is observed (see Fig. 1). Note, that besides the direct fit with equal weight for the amplitudes of all sites, λ can also be determined using the method of asymptotic slope [26]. Here the data is first averaged within shells of fixed distance from $\mathbf{r}_{\max}$ and fitted thereafter. However, using this second approach the detection of the Anderson transition is not as robust and more sensitive to the fluctuations of the data. We therefore refrain from considering corresponding results.

2.2 Inverse participation number

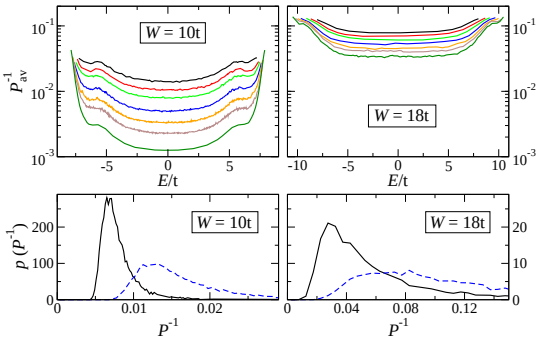


Fig.2 Upper part: Averaged inverse participation number P_{av}^{-1} of 1000 systems with L^3 sites and PBC (top to bottom: $L = 8, 9, 10, 12, 14, 16, 20$). Lower part: Probability density of P^{-1} for the 10^3 system in the band centre (solid line) and near the band edges (dashed line). Note the different scales in the lower panels.

Yet another quantity that measures the Anderson transition is the inverse participation number [27],

$$P^{-1}(E_n) = \sum_{i=1}^{N} |\psi_n(\mathbf{r}_i)|^4 , \tag{4}$$

which is proportional to the inverse number of sites that contribute to a given one-particle wavefunction ψ_n. For delocalised states we find $P^{-1} \sim 1/N$, which vanishes in the thermodynamic limit. Localised states, on the other hand, approximately extend over a finite volume N_0, yielding $P^{-1} \sim 1/N_0$ independently of the system size N. In Fig. 2 this behaviour is demonstrated for small and large disorder W. While in the localised case ($W = 18t$) P^{-1} is almost independent of L, apparently it decreases with L for extended states ($W = 10t$). Apart from the different scaling, the distribution of P^{-1} changes at the transition, being sharply peaked for extended states and rather broad for localised ones (lower part of Fig. 2).

Based on the distribution of the participation number P recently an alternative numerical approach for monitoring the Anderson transition was proposed [28]. In analogy to results for a certain class of power-law random banded matrices, which

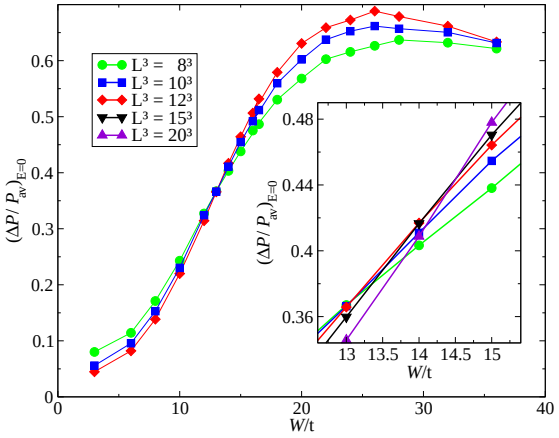


Fig.3 Normalised standard deviation of the participation number in the band centre as a function of disorder for different system sizes using PBC. The obtained results were averaged over 1000 realizations of disorder.

indicate the scale invariance of the distribution of P at the Anderson transition, Malyshev et al. [28] suggest to detect the transition by studying the ratio of the standard deviation of P, ΔP, to the mean participation number $P_{\rm av}$, which should be independent of the system size at the critical disorder.

So far this approach has only been tested for a one-dimensional model with diagonal disorder and power-law long-range hopping [28], which shows a transition at the band edge and can thus be tackled with the Lanczos method. In Fig. 3 we present first data for the band centre of the standard Anderson model. While for small disorder the ratio $\Delta P/P_{\rm av}$ decreases with increasing system size, at large disorder the opposite happens. The intersection of the curves is not completely independent of the system size (see inset of Fig. 3), and a precise determination of the transition requires some finite size scaling of the data. Performing a finite-size scaling [28] our data is consistent with a critical disorder strength of $W_c \approx 16.1 \pm 0.8$ in the thermodynamic limit.

2.3 Local density of states

Already in his seminal paper [6] Anderson pointed out that in order to describe the transition from delocalised to localised states it is very instructive to discuss the distribution of local quantities of interest, such as the escape rate or recurrence probability from or to a given site. Another suitable quantity that becomes critical at the Anderson transition is the LDOS [12, 29],

$$\rho_i(E) = \sum_{n=1}^{N} |\psi_n(\mathbf{r}_i)|^2 \delta(E - E_n)\,, \tag{5}$$

which for a given energy directly measures the local amplitude of the wavefunction at site $\mathbf{r}_i$. So far the LDOS has been considered mainly within analytical approaches or by the Lanczos recursion method [29]. Typically the latter suffers from severe stability problems at high expansion order and conclusive results for the Anderson transition are difficult to obtain [30]. Fortunately the KPM technique [17] described in Appendix A is a very efficient way to circumvent these difficulties and allows the

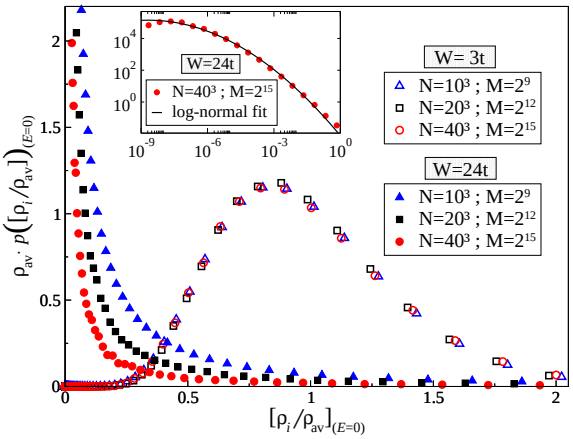


Fig.4 General shape and finite size scaling of the LDOS distribution $p(\rho_i/\rho_{\mathrm{av}})$. Keeping the ratio $N/M = 1.95$ fixed for $N = 10^3, 20^3, 40^3$ and $K_r \times K_s = 10^4\times100,\ 100\times100,\ 32\times32$ respectively, we calculated histograms for $E \in [-0.1t, 0.1t]$. Inset: Double logarithmic plot of $p(\rho_i/\rho_{\mathrm{av}})$ for the localised case together with a log-normal fit to the data.

calculation of high-resolution LDOS data for very large systems. In a nutshell, within this approach the function of interest is expanded in a finite series of Chebyshev polynomials. To weaken the effects of the truncation and ensure properties such as positivity and normalisation, the function is convoluted with an appropriate integral kernel. The resolution of the method is inversely proportional to the order of the expansion M (the number of so-called Chebyshev moments).

Adopting Anderson's original point of view that a proper description of disordered systems should focus on distribution functions, we calculated $\rho_i(E)$ for a large number of samples, K_r, and sites, K_s, and studied its statistical properties. In Figure 4 we show the resulting distribution of $\rho_i(E=0)$, normalised by its mean value ρ_{av}, for two characteristic values of disorder. As ρ_{av} is a function of disorder, this normalisation ensures $\langle \rho_i/\rho_{\mathrm{av}} \rangle = 1$ independent of W, allowing thus an appropriate comparison. In the delocalised phase, $W = 3t$, the distribution is rather symmetric and peaked close to its mean value. Note that increasing the system size and the expansion order, such that the ratio of mean level spacing and KPM resolution is fixed, does not change the distribution. This is in strong contrast to the localised phase, e.g., $W = 24t$, where the distribution of $\rho_i(E)$ is extremely asymmetric. Although most of the weight is now concentrated close to zero, the distribution extends to very large values of ρ_i, causing the mean value to be much larger than the most probable value. In addition, a similar finite size scaling increases the asymmetry and underlines the singular behaviour expected in the thermodynamic limit and at infinite resolution. Note also, that the distribution of the LDOS is well approximated by a log-normal distribution [31],

$$p(x) = \frac{1}{\sqrt{2\pi\sigma^2}} \frac{1}{x} \exp\left(-\frac{\left(\ln\left(x/x_0\right)\right)^2}{2\sigma^2} \right) , \tag{6}$$

as illustrated in the inset of Fig. 4.

Of course, the study of entire distributions is a bit inconvenient, and for practical calculations, instead, we will prefer an appropriate statistics that uniquely characterises the distribution. The above findings suggest, that such a statistics is given by the arithmetic and geometric averages of $\rho_i(E)$,

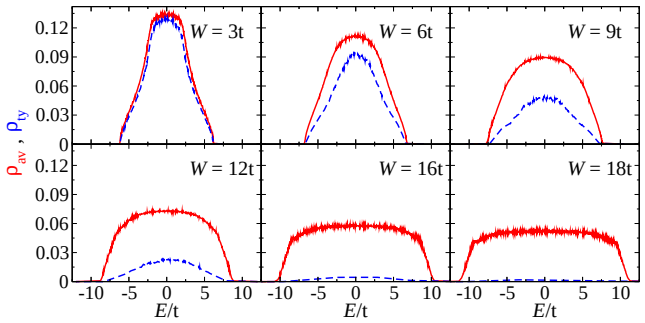


Fig.5 Average (solid line) and typical (dashed line) DOS for a 50^3 lattice with PBC. $K_s \times K_r = 32 \times 32$, $M = 8192$.

$$\rho_{\mathrm{av}}(E) = \frac{1}{K_r K_s} \sum_{k=1}^{K_r} \sum_{i=1}^{K_s} \rho_i(E)\,, \tag{7}$$

$$\rho_{\mathrm{ty}}(E) = \exp\left(\frac{1}{K_r K_s} \sum_{k=1}^{K_r} \sum_{i=1}^{K_s} \ln\big(\rho_i(E)\big) \right)\,. \tag{8}$$

On the one hand, the arithmetic mean for large enough K_r and K_s converges to the standard density of states $\rho(E) = \sum_{n=1}^{N} \delta(E - E_n)$, which is not critical at the Anderson transition. The geometric mean, on the other hand, represents the typical value of the distribution, which, as shown above, is finite in the delocalised phase, but goes to zero in the localised phase. As can be seen from Fig. 5, $\rho_{\mathrm{av}}(E)$ and $\rho_{\mathrm{ty}}(E)$ are almost equal for extended states, whereas for localised states $\rho_{\mathrm{ty}}(E)$ vanishes and $\rho_{\mathrm{av}}(E)$ remains finite. This implies, that the ratio of these two quantities, the normalised typical density of states

$$R(E) := \frac{\rho_{\mathrm{ty}}(E)}{\rho_{\mathrm{av}}(E)}\,, \tag{9}$$

can serve as an order parameter for the Anderson transition with $R > 0$ for extended states and $R = 0$ for localised ones. As for most numerical calculations the transition

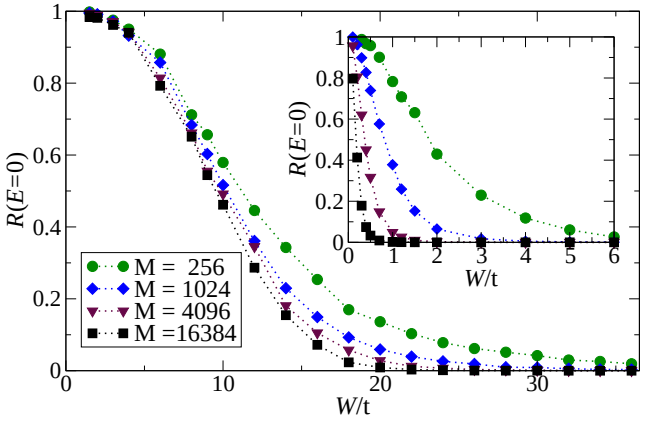


Fig.6 Normalised typical DOS as a function of disorder calculated with increasing expansion order on a 50^3 lattice. The inset shows the corresponding behaviour of the 1d system with 125000 sites. $K_s \times K_r = 32 \times 32$.

is slightly washed out by the finite size of the considered cluster, and by the KPM

resolution. However, for large clusters and increasing M a plot of the ratio R versus disorder strength W (see Fig. 6) allows for a reliable determination of the critical disorder W_c, and, e.g., in the band centre we obtain $W_c(E=0) \simeq 16.5t$ in accordance with other numerical results for the 3d Anderson model [5, 32, 33]. The quality of this criterion is underlined also by our data for a 1d system shown in the inset of Fig. 6. Here, as mentioned above, arbitrarily small disorder leads to localisation of the entire spectrum. Clearly, in our approach this is reflected by a typical DOS that vanishes for large M.

2.4 Comparison of the different methods

Comparing the value of the critical disorder obtained by the various methods discussed in the previous sections, the two main results are the following: (i) As can be seen from Fig. 7, the established criteria and methods show an uncertainty of the critical value W_c in the order of $\pm 0.5t$, which is mainly due to the finite system sizes accessible to the numerical calculations. Note that our data widely agrees with the results in the literature [5, 34]. (ii) The value $W_c \simeq 16.5t$ can be reproduced with the same accuracy using a vanishing typical DOS as an indicator for localisation. An improvement of the accuracy of this result can in principle be obtained by extending the numerical effort (larger systems, higher resolution, high-performance computers), which is facilitated by the straightforward parallelisability of the KPM algorithm. On the other hand, an appropriate scaling ansatz may improve the estimate of W_c on the basis of the presented data.

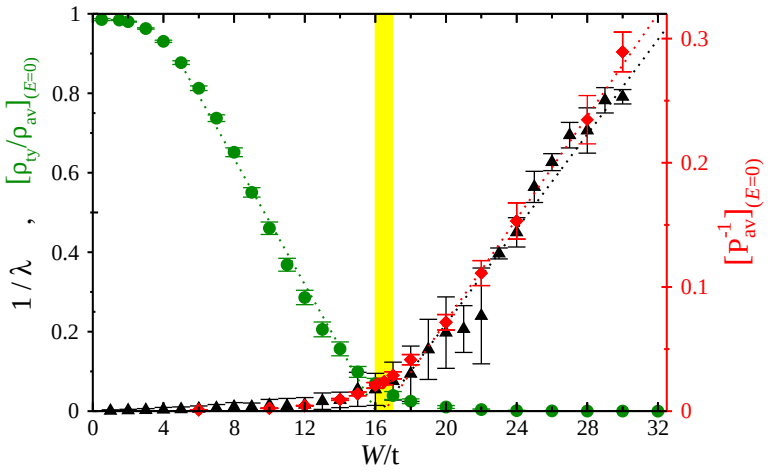


Fig.7 Comparison of the critical values of disorder, W_c, obtained by the methods outlined in Secs. 2.1-2.3. Decay of the wavefunction (triangles): $N = 20^3$ and 30^3, $E_n \in [-0.01, 0.01]$, $K_r = 10$. Average inverse participation number (diamonds): $N = 16^3$, $E_n \in [-0.1, 0.1]$, $K_r = 100$. Normalised typical DOS (circles): $N = 50^3$, $M = 16384$, $K_r \times K_s = 32 \times 32$.

Using the well-established value $W_c(E=0) \simeq 16.5t$ as a calibration of the critical R, required to distinguish localised from extended states for the used values of N and M, we reproduce the mobility edge in the energy-disorder plane [5, 33] using $R_c \simeq 0.05$ (see Fig. 8). We also find the well-known reentrant behaviour near the unperturbed band edges [32, 35]: Varying W for some fixed values of E ($6t < E \leq 7.6t$) a region of extended states separates two regions of localised states. The Lifshitz boundaries, shown as dashed lines, indicate the energy range, where eigenstates are in principle allowed. As the probability of reaching the Lifshitz boundaries is exponentially small, we cannot expect to find states near these boundaries for the finite ensembles considered in any numerical calculation.

With respect to numerical resources, clearly, the methods that are based on a complete diagonalisation of the Hamiltonian (decay of the wavefunction or participation number) are the least favourable ones, since their CPU requirements scale as N^3 and the memory as N^2. Using LAPACK [36] routines for dense matrices on a standard PC-system diagonalisations are feasible for systems up to 21^3. Banded matrix routines together with the bandwidth reduction described in Appendix B allow to increase this size to 30^3.

The calculation of the LDOS via KPM is based on sparse matrix vector multiplications, whose CPU and memory requirements scale only linearly in N. Hence, systems up to 100^3 can be easily handled with desktop computers, and the use of high-performance environments permits the study of even larger ensembles and systems. We conclude that the new method substantially increases the size of numerically accessible systems, which may lead to a more thorough understanding of the Anderson transition.

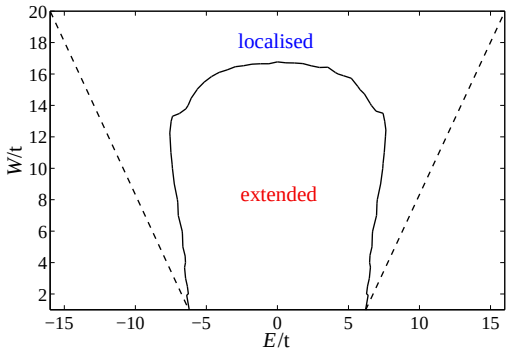


Fig.8 Phase diagram of the Anderson model on a 3d cubic lattice. Shown are the mobility edge (solid curve) as well as the Lifshitz boundaries (dashed lines).

3 Conclusions

With this contribution we aimed to compare well-established numerical localisation criteria for electrons in disordered systems with a recently proposed approach that is based on the evaluation of the typical density of states.

Considering the 3d cubic Anderson model we proved that the local DOS can be very efficiently calculated using a Chebyshev expansion with kernel polynomial re-

finement. Given the numerically obtained distribution of the LDOS, the corresponding typical DOS allows for the detection of the delocalisation-localisation transition with a precision that is comparable to results known from other methods. Like for all numerical schemes, the method is restricted to finite systems, and the obtained critical values are subjected to finite-size effects. However, the low computational resources required by our approach substantially increases the accessible system sizes.

Finally we established the use of the typical DOS as a kind of order parameter, which is important in view of its application to interacting disordered systems.

The authors greatly acknowledge support from the Competence Network for Technical/Scientific High-Performance Computing in Bavaria (KONWIHR). Special thanks go to LRZ München, NIC Jülich and HLRN (Zuse-Institut Berlin) for granting resources on their computing facilities. Discussions with A. Alvermann, F.X. Bronold, S.A. Trugman and W. Weller were greatly appreciated.

A Calculation of the LDOS via the kernel polynomial method

At first glance, Eq. (5) suggests that the calculation of the LDOS could require a complete diagonalisation of H. It turns out, however, that an expansion of ρ_i in terms of Chebyshev polynomials $T_n(x) = \cos(n \arccos x)$ allows for an incredibly precise approximation. Since the Chebyshev polynomials form an orthogonal set on the interval $[-1, 1]$, prior to an expansion the Hamiltonian H needs to be rescaled,

$$\mathfrak{X} = \frac{H}{W/2 + 2dt + 0.01t} \,. \tag{10}$$

Here $W/2 + 2dt$ reflects half the bandwidth of the Anderson model and $0.01t$ is an additional offset that ensures numerical stability of the expansion. In terms of the coefficients

$$\mu_m = \int_{-1}^{1} \rho_i(x) T_m(x)\, dx = \sum_{n=1}^{N} \langle i|n\rangle \langle n|T_m(x_n)|i\rangle = \langle i|T_m(\mathfrak{X})|i\rangle \tag{11}$$

the approximate LDOS $\tilde{\rho}_i(x)$ reads

$$\tilde{\rho}_i(x) = \frac{1}{\pi\sqrt{1-x^2}} \left(g_0\mu_0 + 2\sum_{m=1}^{M} g_m \mu_m T_m(x) \right) . \tag{12}$$

The factors

$$g_m = \frac{1}{M+1} \left((M-m+1)\cos(m\phi) + \frac{\sin(m\phi)}{\tan(\phi)} \right) , \tag{13}$$

where $\phi = \pi/(M+1)$, result from a convolution of the finite series with the so-called Jackson kernel [17], which mainly damps out the Gibbs oscillations known

from polynomial approximations (cf. Fig. 9). The width of the kernel, $\Delta x = \pi/M$, scales inversely with the order of the expansion M and defines the resolution of the method.

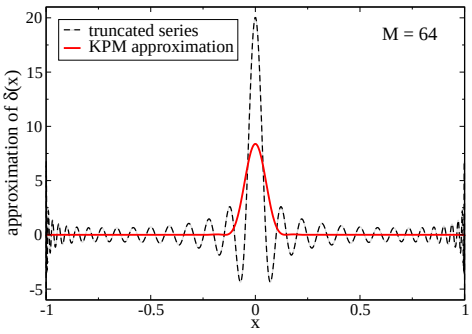


Fig.9 Chebyshev expansion of a δ-peak: The plain truncated series of order $M = 64$ is a strongly oscillating curve (dashed). By convolution with the Jackson kernel it transforms into a strictly positive, well localised peak at $x = 0$ (solid), which is much closer to our usual notion of $\delta(x)$.

Using the recursion relations of the Chebyshev polynomials,

$$T_{m+1}(x) = 2xT_m(x) - T_{m-1}(x)\,, \tag{14}$$

the moments μ_m can be calculated iteratively. An additional trick allows for the generation of two moments with each matrix vector multiplication by $\mathfrak{X}$,

$$\begin{aligned} \mu_{2m-1} &= \sum_{i=1}^{N} 2\langle i|T_m(\mathfrak{X})T_{m-1}(\mathfrak{X})|i\rangle - \mu_1\,, \\ \mu_{2m} &= \sum_{i=1}^{N} 2\langle i|T_m(\mathfrak{X})T_m(\mathfrak{X})|i\rangle - \mu_0\,, \end{aligned} \tag{15}$$

reducing the numerical effort by another factor 1/2. Note that the algorithm requires storage only for the sparse matrix $\mathfrak{X}$ and two vectors of the corresponding dimension.

B Reduction of the bandwidth of the Anderson matrix

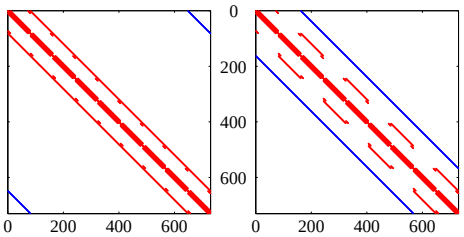


Fig.10 Sparsity pattern of the Anderson matrix. Left: Standard Anderson matrix for a 9^3 system with PBC. The use of DSBEV would require the storage of 648 off-diagonals. Right: Reduced matrix after transformation (16). Only 162 off-diagonals have to be stored.

While for Krylov sub-space methods [37] (like Lanczos or Jacobi-Davidson) we can take advantage of the sparsity of the tight-binding type matrices, the full diagonalisation with LAPACK routines requires their complete storage. Unfortunately,

for periodic boundary conditions the cyclic tridiagonal structure of the matrices spoils the use of band matrix routines like DSBEV. For a L^3-system there are non-vanishing matrix elements in a distance of $L^3 - L^2$ from the diagonal (Fig. 10). Thus almost all matrix elements (most of them zero) need to be stored, giving no advantage compared to full matrix diagonalisation routines like DSYEV.

For linear systems there are tricks to use tridiagonal matrices instead of the corresponding cyclic tridiagonal matrices, which are based on the use of the Sherman-Morrison formula [38]. We are not aware of similar ideas for eigenvalue problems. It turns out, however, that an appropriate sequence of Givens rotations [38] allows the transformation of the cyclic tight-binding matrix (with quadratic blocks close to the outer edges) onto a matrix with blocks only along five diagonals. The corresponding transformation reads

$$H_{\mathrm{red}} = T^T H T \,, \tag{16}$$

where $T = P \otimes \mathbb{1}_{L^2 \times L^2}$ and for odd L the $L \times L$ matrix P is given by

$$P = \frac{1}{\sqrt{2}} \begin{pmatrix} \sqrt{2} & 0 & \dots & \dots & \dots & 0 \\ 0 & -1 & 1 & 0 & \dots & 0 \\ 0 & \dots & 0 & -1 & 1 & 0 \\ \dots & \dots & \dots & \dots & \dots & \dots \\ 0 & \dots & \dots & 0 & -1 & 1 \\ 0 & \dots & \dots & 0 & 1 & 1 \\ \dots & \dots & \dots & \dots & \dots & \dots \\ 0 & \dots & 0 & 1 & 1 & 0 \\ 0 & 1 & 1 & 0 & \dots & 0 \end{pmatrix} . \tag{17}$$

For even L the first row and column are absent.

The bandwidth of H can thus be substantially reduced (to $2L^2$, see Fig. 10), which allows for the full diagonalisation of systems up to 30^3 sites on PC-systems with a memory of 512 MB. Furthermore, the sparsity of the transformation (16) can be used to avoid an explicit matrix-matrix multiplication [39]. Hence the change from H to H_{red} is not time consuming. The advantage of the transformation is not primarily a gain in CPU time but storage.

References

1. D. J. Thouless, Physics Reports **13**, 93 (1974).
2. F. J. Wegner, Z. Phys. B **25**, 327 (1976).
3. P. A. Lee and T. V. Ramakrishnan, Rev. Mod. Phys. **57**, 287 (1985).
4. D. Vollhardt and P. Wölfle, in *Electronic Phase Transitions*, edited by W. Hanke and Y. V. Kopaev, North Holland, Amsterdam, (1992), p. 1.
5. B. Kramer and A. Mac Kinnon, Rep. Prog. Phys. **56**, 1469 (1993).
6. P. W. Anderson, Phys. Rev. **109**, 1492 (1958).
7. J. Fröhlich, F. Martinelli, E. Scoppola and T. Spencer, Commun. Math. Phys. **101**, 21 (1985).
8. R. E. Borland, Proc. Roy. Soc. London, Ser. A **274**, 529 (1963).
9. N. F. Mott and W. D. Twose, Adv. Phys. **10**, 107 (1961).
10. E. Abrahams, P. W. Anderson, D. C. Licciardello and T. V. Ramakrishnan, Phys. Rev. Lett. **42**, 673 (1979).

11. M. Janssen, Physics Reports **295**, 1 (1998).
12. V. Dobrosavljević, A. A. Pastor and B. K. Nikolić, Europhys. Lett. **62**, 76 (2003);
13. V. Dobrosavljević and G. Kotliar, Phys. Rev. Lett. **78**, 3943 (1997).
14. F. X. Bronold and H. Fehske, Phys. Rev. B **66**, 073102 (2002);
15. F. X. Bronold, A. Alvermann, and H. Fehske, Philos. Mag. **84**, 673 (2004).
16. R. Abou-Chacra, P. W. Anderson and D. J. Thouless, J. Phys. C **6**, 1734 (1973).
17. R. N. Silver, H. Röder, A. F. Voter and D. J. Kress, J. of Comp. Phys. **124**, 115 (1996);
18. R. N. Silver and H. Röder, Phys. Rev. E **56**, 4822 (1997).
19. K. Byczuk, W. Hofstetter, and D. Vollhardt, URL`http://arXiv.org/abs/cond-mat/0403765`.
20. G. Schubert, A. Weiße and H. Fehske, URL `http://arXiv.org/abs/cond-mat/0406212`, to appear in Physica B (2005).
21. G. Schubert, A. Weiße and H. Fehske, URL`http://arXiv.org/abs/cond-mat/0406750`.
22. A. Alvermann, G. Schubert, A. Weße, F. X. Bronold and H. Fehske, URL `http://arXiv.org/abs/cond-mat/0406051`, to appear in Physica B (2005).
23. A. Mac Kinnon and B. Kramer, Z. Phys. B **53**, 1 (1983).
24. J. L. Pichard and G. Sarma, J. Phys. C **14**, L127 (1981).
25. I. V. Plyushchay, R. A. Römer, and M. Schreiber, Phys. Rev. B **68**, 064201 (2003).
26. B. J. Last and D. J. Thouless, J. Phys. C **7**, 699 (1974).
27. F. Wegner, Z. Phys. B **36**, 209 (1980).
28. A. V. Malyshev, V. A. Malyshev and F. Domínguez-Adame, URL `http://arXiv.org/abs/cond-mat/0303092`.
29. R. Haydock and R. L. Te, Phys. Rev. B **49**, 10845 (1994).
30. W. T. Arnold and R. Haydock, Phys. Rev. B **66**, 155121 (2002).
31. E. W. Montroll and M. F. Shlesinger, J. Stat. Phys. **32**, 209 (1983).
32. B. Bulka, M. Schreiber and B. Kramer, Z. Phys. B **66**, 21 (1987).
33. H. Grussbach and M. Schreiber, Phys. Rev. B **51**, 663 (1995).
34. B. Kramer, K. Broderix, A. Mac Kinnon and M. Schreiber, Physica A **167**, 163 (1990).
35. S. L. A. de Queiroz, Phys. Rev. B **653**, 214202 (2001).
36. *The Linear Algebra PACKage*, URL `http://www.netlib.org`.
37. Y. Saad, *Numerical Methods for Large Eigenvalue Problems* (University Press, Manchester, 1992).
38. W. H. Press, B. P. Flannery, S. A. Teukolsky and W. T. Vetterling, *Numerical Recipes* (Cambridge University Press, Cambridge, 1986).
39. G. Schubert, diploma thesis, Universität Bayreuth (2003).